

Photo-Disintegration of the Iron Nucleus in Fractured Magnetite Rocks with Magnetostriction

A. Widom and J. Swain

Physics Department, Northeastern University, Boston MA USA

Y.N. Srivastava

Physics Department & INFN, University of Perugia, Perugia IT

There has been considerable interest in recent experiments on iron nuclear disintegrations observed when rocks containing such nuclei are crushed and fractured. The resulting nuclear transmutations are particularly strong for the case of magnetite rocks, i.e. loadstones. We argue that the fission of the iron nucleus is a consequence of photo-disintegration. The electro-strong coupling between electromagnetic fields and nuclear giant dipole resonances are central for producing observed nuclear reactions. The large electron energies produced during the fracture of piezomagnetic rocks are closely analogous to the previously discussed case of the fracture of piezoelectric rocks. In both cases electro-weak interactions can produce neutrons and neutrinos from energetic protons and electrons thus inducing nuclear transmutations. The electro-strong condensed matter coupling discussed herein represents new many body collective nuclear photo-disintegration effects.

PACS numbers: 62.20.mm, 81.40.Np, 03.75.Be, 14.20.Dh

I. INTRODUCTION

Recent measurements of nuclear reactions[1-3] that accompany the fracturing[4-7] of piezoelectric and piezomagnetic rocks have inspired a great deal of interest. The contribution of electro-weak processes to the production of neutrons,

$$e^- + p^+ \rightarrow n + \nu_e, \quad (1)$$

during the fracture of piezoelectric rocks has been discussed in previous work[8]. One of the purposes of this work is to expand the theory to include the fracture of rocks[9] with magnetostriction, again employing the conversion of mechanical energy (phonons) to electromagnetic energy (photons) and vice-versa.

Our purpose is also to investigate other sources of nu-

clear radiation, in particular those radiations that are a consequence of electro-strong[10] nuclear fission reactions. To see what is involved, consider the fracture of Fe_3O_4 magnetite rocks, i.e. magnetic semiconductor loadstones. The fracture process accelerates electrons which in turn produce electromagnetic radiation. Such radiation can induce the photo-disintegration of the iron nucleus. The absorption of a photon can cause a transition to an excited compound nuclear state, e.g.

$$\gamma + {}^{56}Fe \rightarrow {}^{56}Fe^*. \quad (2)$$

The quantum electrodynamic excitation to a compound nuclear state is exhibited in the Feynman diagrams of FIG. 1. The photon nuclear vertex coupling is via the iron nucleus giant dipole resonance[11]. The strong interactions control the decay of the compound nucleus

$${}^{56}Fe^* \rightarrow (\text{fission products}). \quad (3)$$

In general terms, the photo-disintegration of nuclei is presently well understood.

In Sec.II the giant dipole resonant coupling to the electromagnetic field is reviewed. The total cross section for absorbing the photon in FIG. 1 (a) has a peak value of

$$\sigma_0 = 4\pi Z\alpha \left(\frac{\hbar}{M\Gamma} \right), \quad (4)$$

wherein $Z = 26$ is the number of protons in the iron nucleus, the quantum electrodynamic coupling strength is $\alpha = (e^2/\hbar c) \approx 1/137.036$, the proton mass is M and the fission decay rate of the compound nucleus in Eq.(3) is Γ . The silicon and aluminum photo-disintegration fission channels are briefly discussed in Sec.III.

In Sec.IV we consider the retarding force

$$\vec{F} = -\frac{dE}{dx}, \quad (5)$$

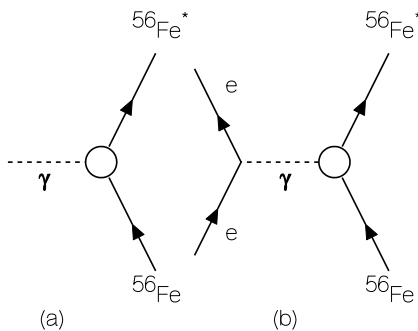


FIG. 1: Shown in (a) is the Feynman diagram for producing an excited compound nucleus from a real Bremsstrahlung photon. Shown in (b) is a similar process due to an incident electron exchanging a virtual photon with the nucleus.

or energy loss per unit length for an energetic electron passing through magnetite. The ratio of how much energy dE is lost to other electrons in atomic transitions and how much energy $d\tilde{E}$ is lost to giant dipole excitations of the compound nucleus is computed in detail. Formally, the energy transfer efficiency $\eta = (d\tilde{E}/dE) \sim 1\%$.

In Sec.V a theoretical explanation is provided for the experimental evidence that fracturing loadstones produces photo-disintegration fission products of ^{56}Fe nuclei. The elastic energy of mesoscopic microcrack production during a fracture ultimately yields a major macroscopic fracture separation. The mechanical energy is converted by magnetostriction into electromagnetic field energy. The electromagnetic field energy decays via radio frequency (microwave) oscillations. The radio frequency fields accelerate the condensed matter electrons which then collide with nuclei producing fission products on the surfaces of these microcracks. In the concluding Sec.VI, the nature of fission microcrack wall remnants are discussed.

II. GIANT DIPOLE RESONANCE

Let $|0\rangle = |^{56}\text{Fe}\rangle$ represent the ground state internal wave function of the iron nucleus. Representing the dipole approximation for the interaction in FIG. 1,

$$H_{\text{int}} = -\mathbf{E} \cdot \mathbf{d}, \quad (6)$$

the nuclear polarizability

$$\beta(\zeta) = \frac{i}{3\hbar} \int_0^\infty e^{i\zeta t} \langle 0 | \mathbf{d}(t) \cdot \mathbf{d}(0) - \mathbf{d}(0) \cdot \mathbf{d}(t) | 0 \rangle dt. \quad (7)$$

The ground state of the ^{56}Fe nucleus has zero spin. The polarizability is thereby an isotropic tensor.

A. Photon Cross Sections

The elastic photon scattering amplitude for

$$\gamma + ^{56}\text{Fe} \rightarrow \gamma + ^{56}\text{Fe} \quad (8)$$

is given by

$$\mathcal{F}_{fi}(\omega) = \left(\frac{\omega}{c}\right)^2 \beta(\omega + i0^+) \mathbf{e}_f^* \cdot \mathbf{e}_i \quad (9)$$

wherein $\mathbf{e}_{i,f}$ are, respectively, the initial and final photon polarization vectors and ω is the photon frequency. The elastic photon cross section is thereby

$$\begin{aligned} \sigma_{\text{el}}(\omega) &= \frac{1}{2} \sum_f \sum_i \int |\mathcal{F}_{fi}(\omega)|^2 d\Omega_f, \\ \sigma_{\text{el}}(\omega) &= \frac{8\pi}{3} \left(\frac{\omega}{c}\right)^4 |\beta(\omega + i0^+)|^2. \end{aligned} \quad (10)$$

wherein we have averaged over initial polarization states and summed over final polarization states. The total cross section follows from the optical theorem

$$\begin{aligned} \sigma_{\text{tot}}(\omega) &= \left(\frac{4\pi c}{\omega}\right) \Im m \mathcal{F}_{ii}(\omega), \\ \sigma_{\text{tot}}(\omega) &= \left(\frac{4\pi\omega}{c}\right) \Im m \beta(\omega + i0^+). \end{aligned} \quad (11)$$

The inelastic cross section $\sigma_{\text{in}}(\omega)$ for the central reaction

$$\gamma + ^{56}\text{Fe} \rightarrow ^{56}\text{Fe}^* \rightarrow (\text{fission products}) \quad (12)$$

follows from Eqs.(10) and (11) via the sum rule

$$\sigma_{\text{tot}}(\omega) = \sigma_{\text{el}}(\omega) + \sigma_{\text{in}}(\omega). \quad (13)$$

B. Dispersion Relations

From Eq.(7), it is expected that the nuclear polarizability obey a dispersion relation for $\Im m \zeta > 0$ of the form

$$\beta(\zeta) = \frac{2}{\pi} \int_0^\infty \left[\frac{\omega \Im m \beta(\omega + i0^+) d\omega}{\omega^2 - \zeta^2} \right]. \quad (14)$$

With

$$\hbar\omega_{n0} = E_n - E_0 \quad \text{and} \quad \mathbf{d}_{n0} = \langle n | \mathbf{d} | 0 \rangle, \quad (15)$$

we have

$$\Im m \beta(\omega + i0^+) = \frac{\pi}{3\hbar} \sum_n |\mathbf{d}_{n0}|^2 \delta(\omega - \omega_{n0}) \quad (16)$$

For example, the static polarizability of the nucleus is given by

$$\beta = \lim_{\zeta \rightarrow i0^+} \beta(\zeta) = \frac{2}{\pi} \int_0^\infty \Im m \beta(\omega + i0^+) \frac{d\omega}{\omega}. \quad (17)$$

Employing Eq.(6) in second order perturbation theory

$$\begin{aligned} \frac{1}{2} \beta |\mathbf{E}|^2 &= \sum_n \frac{|\langle n | H_{\text{int}} | 0 \rangle|^2}{E_n - E_0}, \\ \beta &= \frac{2}{3\hbar} \sum_n \frac{|\mathbf{d}_{n0}|^2}{\omega_{n0}}. \end{aligned} \quad (18)$$

For a nucleus of charge Z , the equal time commutation relation

$$\frac{i}{3\hbar} (\dot{\mathbf{d}} \cdot \mathbf{d} - \mathbf{d} \cdot \dot{\mathbf{d}}) = \frac{Ze^2}{M}, \quad (19)$$

wherein M is the proton mass, yields in virtue of Eqs.(7) and (19) the large frequency limit

$$\lim_{|\zeta| \rightarrow \infty} \zeta^2 \beta(\zeta) = - \left(\frac{Ze^2}{M} \right). \quad (20)$$

Eqs.(14) and (20) imply the sum rule[12–14]

$$\frac{2}{\pi} \int_0^\infty \omega \Im m \beta(\omega + i0^+) d\omega = \frac{Ze^2}{M}, \quad (21)$$

or equivalently

$$\int_0^\infty \sigma_{\text{tot}}(\omega) d\omega = 2\pi^2 \left(\frac{Ze^2}{Mc} \right) = 2\pi^2 Z\alpha \left(\frac{\hbar}{M} \right). \quad (22)$$

The above dispersion relation and sum rule are implemented in simple nuclear giant dipole resonant models.

C. Single Giant Resonance Model

The most simple model for discussing the nuclear giant dipole resonance involves a single damped harmonic oscillator with resonant frequency ω_0 and damping coefficient Γ .

$$\beta(\zeta) = \frac{Ze^2}{M(\omega_0^2 - \zeta^2 - i\zeta\Gamma)}. \quad (23)$$

Eqs.(11) and (23) then imply a total cross section

$$\begin{aligned} \sigma_{\text{tot}}(\omega) &= \left(\frac{4\pi Ze^2}{Mc} \right) \left[\frac{\omega^2 \Gamma}{(\omega_0^2 - \omega^2)^2 + \omega^2 \Gamma^2} \right], \\ \sigma_{\text{tot}}(\omega) &= \sigma_0 \left[\frac{\omega^2 \Gamma^2}{(\omega_0^2 - \omega^2)^2 + \omega^2 \Gamma^2} \right], \\ \sigma_0 &= \left(\frac{4\pi Ze^2}{Mc\Gamma} \right) = 4\pi Z\alpha \left(\frac{\hbar}{M\Gamma} \right). \end{aligned} \quad (24)$$

The single resonance Eq.(24) is plotted in FIG. 2.

D. Model Parameters

In the Migdal theory[15, 16] of the nuclear Landau-Fermi liquid, an isotopic spin zero sound mode of velocity c_0 confined to a spherical cavity has a frequency

$$\omega_0 = \frac{zc_0}{R} \quad (\text{with the lowest root of } z = \tan z > 0). \quad (25)$$

The radii of nuclei obey

$$R \approx r_0 A^{1/3} \quad \text{wherein } r_0 \approx 1.2 \text{ fm}. \quad (26)$$

With the ratio of zero sound speed to light speed given by $(c_0/c) \approx 0.1$ we then have the prediction

$$\hbar\omega_0 \approx \frac{70 \text{ MeV}}{A^{1/3}} \Rightarrow \hbar\omega_0(^{56}\text{Fe}) \approx 20 \text{ MeV}. \quad (27)$$

Since the Landau-Fermi liquid theory gives rise to the complex zero sound mode frequency $\varpi = c_0 k - (i/2)Dk^2$ as $k \rightarrow 0$, the width of the zero sound resonance must have the form

$$\Gamma = D \left(\frac{\omega_0}{c_0} \right)^2 = \frac{z^2 D}{R^2} = \frac{\Gamma_0}{A^{2/3}} \quad (28)$$

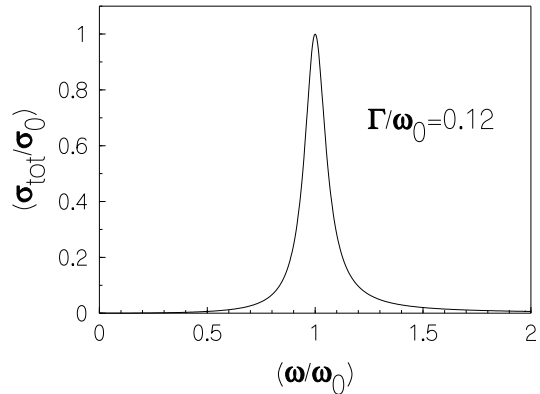


FIG. 2: Shown is the total cross section employing a single nuclear dipole giant resonance model according to Eq.(24). The resonant energy for creating a compound nucleus is $\hbar\omega_0$ as in Eq.(2). The transition rate is Γ for the compound nucleus to decay into fission products as in Eq.(3). The peak cross section is $\sigma_0 = 4\pi Z\alpha\hbar/M\Gamma$. The resonant width $\Gamma \approx 0.12 \omega_0$ for ^{56}Fe is only approximate.

wherein

$$\Gamma_0 = \left(\frac{z^2 D}{r_0^2} \right). \quad (29)$$

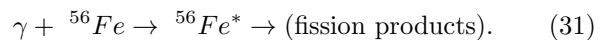
Thus,

$$\frac{\Gamma}{\omega_0} = \left(\frac{zD}{c_0 r_0} \right) \frac{1}{A^{1/3}} \approx \frac{0.5}{A^{1/3}}. \quad (30)$$

The above estimates are semi-quantitative but to the best of our knowledge are new.

III. DISINTEGRATION FISSION CHANNELS

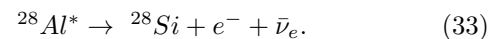
In the photo-disintegration of iron



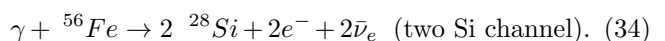
one should consider the silicon and aluminum fission products within the prominent decay channels. If in accordance with the liquid drop model, the decay of the compound excited nucleus $^{56}\text{Fe}^*$ is preferentially into two equal excited aluminum droplets, the decay reads



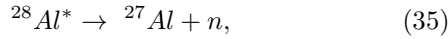
Each of the resulting aluminum nuclei, then undergoes the weak decay



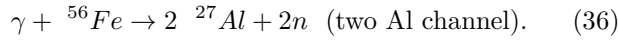
Altogether,



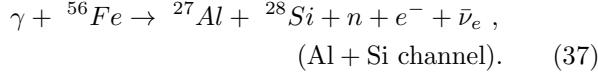
If two neutrons evaporate from each of the two resulting aluminum nuclei



then a possible channel is



A third channel is evidently



In terms of the branching ratio,

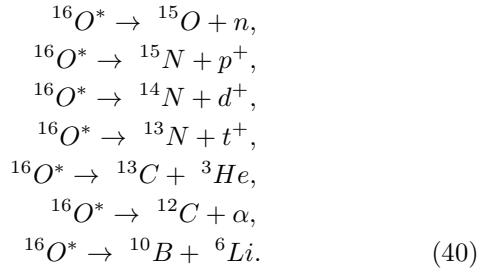
$$b = \frac{\Gamma({}^{28}\text{Al}^* \rightarrow {}^{28}\text{Si} + e^- + \bar{\nu}_e)}{\Gamma({}^{28}\text{Al}^* \rightarrow {}^{27}\text{Al} + n)}, \quad (38)$$

one should be able to compute the branching ratio of the above three fission products.

In magnetite Fe_3O_4 , there will also be the photo-disintegration of the ${}^{16}\text{O}$ nucleus,



Possible fission channels are thereby



The photo-disintegration of oxygen gives rise to diverse types of nuclear radiation.

IV. RETARDATION FORCES

Consider a beam of electrons each having an energy

$$E = mc^2\gamma = \frac{mc^2}{\sqrt{1 - (v/c)^2}}. \quad (41)$$

passing through magnetite. The energy loss per unit length for the electron is the retarding force

$$F = -\frac{dE}{dx}. \quad (42)$$

If the fast electron causes other electrons to undergo atomic transitions, then the retarding force takes on the well known form[17]

$$F = \left(\frac{4\pi ne^4}{mv^2}\right) \left[\ln\left(\frac{mv^2\gamma^2}{\hbar\omega_i}\right) - \left(\frac{v}{c}\right)^2 \right], \quad (43)$$

wherein $\hbar\omega_i$ is the log mean ionization energy of an atom and n is the density of electrons per unit volume.

For \tilde{n} iron ${}^{56}\text{Fe}$ nuclei per unit volume, the retardation force due to the giant dipole resonance at frequency ω_0 in iron is given by

$$\tilde{F} = \left(\frac{4\pi\tilde{n}Z^2e^4}{Mv^2}\right) \left[\ln\left(\frac{Mv^2\gamma^2}{\hbar\omega_0}\right) - \left(\frac{v}{c}\right)^2 \right], \quad (44)$$

wherein M is the proton mass.

The photo-disintegration efficiency may be defined as

$$\eta = \left(\frac{\tilde{F}}{F}\right) = \left(\frac{d\tilde{E}}{dE}\right), \quad (45)$$

wherein $d\tilde{E}$ is the energy transferred from a fast electron to fission products and dE is the energy transferred from a fast electron to atomic electronic transitions. The ratio of the energy excitations is small ($\omega_i/\omega_0 \sim 10^{-7}$). Eqs.(43), (44) and (45) imply for $\gamma \gg 1$

$$\eta \approx \left(\frac{Z^2\tilde{n}m}{nM}\right) \left\{ \frac{\ln[(Mv^2\gamma^2/\hbar\omega_0)] - (v/c)^2}{\ln[(mv^2\gamma^2/\hbar\omega_i)] - (v/c)^2} \right\}. \quad (46)$$

Typically, the nuclear yield is as expected of the order of $\eta \sim 1\%$.

V. FRACTURED MAGNETIC ROCKS

The thermodynamic properties of magnetite Fe_3O_4 are determined by the energy per unit volume $u = u(s, \mathbf{w}, \mathbf{H})$ wherein s is the entropy per unit volume, \mathbf{w} is the strain and \mathbf{H} is the magnetic intensity

$$du = Tds + \sigma : d\mathbf{w} - \mathbf{M} \cdot d\mathbf{H}. \quad (47)$$

Magnetite at room temperature is a ferromagnet. Within a magnetic domain, one may formally define a piezomagnetic coefficient by the thermodynamic derivatives

$$\beta_{i,jk} = \left(\frac{\partial M_i}{\partial w_{jk}}\right)_{s,\mathbf{H}} = -\left(\frac{\partial \sigma_{jk}}{\partial H_i}\right)_{s,\mathbf{w}}. \quad (48)$$

These coefficients describe how strain can induce magnetization and how magnetic intensity can induce stress. Some implications of this conversion from mechanical energy into electromagnetic energy are quite striking. If a solid has an impact on the surface of a magnetostrictive material, then the resulting induced electric fields can measure the nature of the induced impact stress.

The piezomagnetic coefficients describe the conversion of phonons (mechanical vibrations) into magnons (magnetic energy). Since the magnetization yields the current density

$$\mathbf{J}_{\text{mag}} = c \text{curl} \mathbf{M}, \quad (49)$$

Maxwell's equations describe the manner that magnons radiate photons,

$$\mathbf{E}(\mathbf{r}, t) = -\left(\frac{1}{c}\right) \text{curl} \int \frac{\dot{\mathbf{M}}(\mathbf{r}', t - R/c)}{R} d^3\mathbf{r}',$$

$$\text{wherein } R = |\mathbf{r} - \mathbf{r}'| \text{ and } \frac{\partial \mathbf{M}(\mathbf{r}, t)}{\partial t} \equiv \dot{\mathbf{M}}(\mathbf{r}, t). \quad (50)$$

Under conditions of rock crushing[9], the magnetization changes give rise in the microcracks[19] to microwave radiation as given by Eq.(50). Microwaves can in turn give rise to accelerated electrons to an energy γmc^2 . Let us consider this in more detail.

A. Loadstone Fractures

The formation of microcracks during fracture can be formulated in terms of the elastic properties of the solid[20–22]. Let σ_{bond} be the fracture stress calculated on the basis of chemical bonds. The chemical bond stress can be expressed in terms of the elastic properties of the crystal

$$\sigma_{\text{bond}} = \left[\frac{2\mathcal{E}}{\pi(1-\nu^2)} \right], \quad (51)$$

wherein \mathcal{E} is Young's modulus and ν is Poisson's ratio. The experimental tensile stress σ_F of a loadstone obeys

$$\sigma_F \ll \sigma_{\text{bond}} \quad (52)$$

due to the intrinsic surface tension of the microcrack walls.

For loadstone we have the following numerical estimates;

$$\sigma_{\text{bond}} \sim 10^{12} \frac{\text{erg}}{\text{cm}^3} \quad \text{and} \quad \sigma_F \sim 10^{10} \frac{\text{erg}}{\text{cm}^3}. \quad (53)$$

During the time of microcrack formation, the stress within the empty open sliver is determined in order of magnitude by the Maxwell pressure tensor; i.e.

$$\sigma_F \sim \frac{|\mathbf{E}|^2}{4\pi} \Rightarrow |\mathbf{E}|^2 \sim 10^{11} \text{ Gauss}^2. \quad (54)$$

One may now compute the energy of electrons formed near the microcrack walls due to electric field generation.

B. Electron Energy

The rate of change of momentum of an electron in an electric field is given by

$$\frac{d\mathbf{p}}{dt} = e\mathbf{E}. \quad (55)$$

Putting

$$mc^2\gamma = \sqrt{c^4m^2 + c^2|\mathbf{p}|^2}, \quad (56)$$

yields

$$\gamma^2 = 1 + \frac{|\mathbf{p}|^2}{m^2c^2} = 1 + \frac{e^2|\mathbf{E}|^2}{m^2c^2\Omega^2}, \quad (57)$$

wherein Eq.(55) has been invoked and Ω is an effective frequency of electric field fluctuations[8]

$$\frac{1}{\Omega^2} = \frac{\int |\mathbf{E}_\omega|^2 (d\omega/\omega^2)}{\int |\mathbf{E}_\omega|^2 d\omega}. \quad (58)$$

Since

$$\frac{e}{mc} = 1.75882915 \times 10^7 \left(\frac{1}{\text{Gauss sec}} \right), \quad (59)$$

Eqs.(54), (57) and (59) yield

$$\gamma \sim \frac{3 \times 10^{12}/\text{sec}}{\Omega}. \quad (60)$$

For the microwave electromagnetic radiation within the microcrack, $\Omega \sim 10^{10}/\text{sec}$ so that

$$\gamma \sim 300 \Rightarrow \gamma mc^2 \sim 150 \text{ MeV}. \quad (61)$$

Such energetic electrons are perfectly capable of inducing the photo-disintegration of nuclei.

C. Electron Deposition

One can determine the order of magnitude of the number of energetic electrons which arrive on the surface area of a microcrack wall during the formation. If n_s represents the number per unit area of excess electronic charges, then applying Gauss' law to the wall surface yields

$$4\pi en_s = E_\perp, \quad (62)$$

wherein E_\perp is the component of the electric field normal to the surface. Eqs.(54) and (62) yield the electronic deposition density per unit area

$$n_s \sim 3 \times 10^{13}/\text{cm}^2 \quad (63)$$

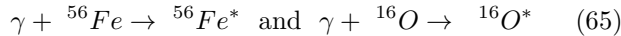
If the yield of nuclear fission events per deposited electron is a few percent, then the density of fission events per unit area on a newly formed microcrack wall is given by

$$\varpi_s \sim \frac{10^{12} \text{ fission events}}{\text{cm}^2} \quad (64)$$

This is a sufficient number of fission events for forming visible patches of monolayer films that would be observable to the eye.

VI. CONCLUSIONS

The recent experimental work on nuclear radiations from fracturing magnetite, $[Fe_2^{++++}][Fe^{++}][O_4^{-}]$, can be largely understood. The theory contains an important electro-strong interaction component. Giant dipole resonances in the iron and oxygen nuclei



give rise to a conferable diversity of fission nuclear radiation from the excited compound nuclear states ${}^{56}Fe^*$ and ${}^{16}O^*$ when rocks containing such nuclei are crushed and fractured. Nuclear transmutations are present in

the fracture of many brittle rocks but they are particularly plentiful for the case of magnetite rocks, i.e. loadstones. The fission events nucleus are a consequence of photo-disintegration. The electro-strong coupling between electromagnetic fields in piezomagnetic rocks are closely analogous to the previously discussed case of the fracture of piezoelectric rocks. In both cases, electro-weak interactions can produce long wavelength neutrons and neutrinos from energetic protons and electrons thus inducing nuclear transmutations. The electro-strong condensed matter coupling discussed herein represents new many body collective nuclear photo-disintegration effects.

-
- [1] A. Carpinteri, O. Borla, G. Lacidogna and A. Manuello, *Physical Mesomechanics* **13**, 268 (2010).
- [2] A. Carpinteri, G. Lacidogna, A. Manuello and O. Borla, *Strength, Fracture and Complexity* **7**, 13 (2011).
- [3] A. Carpinteri and A. Manuello, *Strain Suppl.2* **47**, 267 (2011).
- [4] A. Carpinteri, A. Chiodoni, A. Manuello and R. Sandrone, *Strain Suppl.2* **47**, 282 (2011).
- [5] A. Carpinteri and A. Manuello, *Physical Mesomechanics* **15**, 37 (2012).
- [6] A. Carpinteri, G. Lacidogna, A. Manuello and O. Borla, *Rock Mechanics and Rock Engineering* **45**, 445 (2012).
- [7] A. Carpinteri, G. Lacidogna, O. Borla, A. Manuello and G. Niccolini, *Sadhana* **37**, 59 (2012).
- [8] A. Widom, J. Swain and Y.N. Srivastava, *J. Phys. G: Nucl. Part. Phys.* **G 40**, 015006 (2013).
- [9] S. Koshevaya, V. Grimalsky, N. Makarets, A. Kotsarenko, J. Siquieros-Alatorre, R. Perez-Enriquez and D. Juarez-Romero, *Adv. Geosci.* **14**, 25 (2008).
- [10] J. Swain, A. Widom, Y.N. Srivastava, arXiv:1306.5165 [nucl-th] 19 June (2013).
- [11] K.A. Snover, *Annual Review of Nuclear and Particle Science* **36**, 545 (1986).
- [12] W. Thomas, *Naturwissenschaften* **13**, 627 (1925).
- [13] W. Kuhn, *Z. Phys.* **33**, 408 (1025).
- [14] F. Reiche and W. Thomas, *Z. Phys.* **34**, 510 (1025).
- [15] A. B. Migdal, “*Theory of Finite Fermi-Systems and Properties of the Atomic Nucleus*” John Willey & Sons, New York (1967).
- [16] A.B. Migdal, D.N. Voskresenskii, E.E. Saperstein, and M.A. Troitskii, *Phys. Rep.* **192**, 179 (1990).
- [17] V.B. Berestetskii, E.M. Lifshitz and L.P. Pitaevskii, “*Quantum Electrodynamics*”, page 335, Eq.(82.26), Pergamon Press, Oxford (1980).
- [18] L. Lolloz, S. Pattofatto and O Hubert, *J. of Electrical Engineering* **57**, 15 (2006).
- [19] C. Gruerro, J. Schelbert, D. Bonamy and D. Dolmas, *Proc. Natl. Acad. Sci. USA* **129**, 190 (2012).
- [20] L.D. Landau and E.M. Lifshitz, “*Theory of Elasticity*” Sec.31, Pergamon Press, Oxford(1970).
- [21] L.B. Freund, “*Dynamic Fracture Mechanics*”, Cambridge University Press, Cambridge (1998).
- [22] A.A. Griffith, *Proc. R. Soc.* **221**, 161 (1921).